Available online at www.garmian.edu.krd

Passer Journal

Passer 5 (Issue 2) (2023) 348-355

http://passer.garmian.edu.krd/

Improvement of the Optical Properties of Zn-Doped MnO Nanocomposites Thin films

Adnan Mahmud Saleh[1*]

[1]*Department of Physics, College of Education, University of Garmian, Kalar, Kurdistan Region, Iraq*

Received 19 July 2023; revised 20 August 2023;
accepted 20 August 2023; available online 29 August 2023

DOI: 10.24271/PSR.2023.407846.1349

ABSTRACT

Nanostructured thin films of MnO, Mn:5%ZnO, and Mn:10%ZnO were deposited through the process of chemical spray pyrolysis (CSP) on glass substrates. To examine the structural and optical characteristics, various analytical techniques such as XRD, FE-SEM, and UV-VIS spectrophotometer were employed to characterize the thin films that were synthesized. X-ray diffraction demonstrated that deposition conditions affected crystallite size in these thin films, and the Scherrer equation showed that the average crystalline size increased with ZnO-doped manganese solution. The linear plot shows a positive slope (0.0004 and 0.001) for all samples MnO and Mn:10%ZnO, which have a tensile strain and a lattice expansion in nano-tetragonal samples, except for Mn:5%ZnO, which has a negative slope (-0.0013). FE-SEM images showed that the particle size for all samples was 35.7, 56.9, and 23.6 nm for MnO, Mn:5%ZnO, and Mn:10%ZnO nanostructured thin films, respectively, which matches XRD analyses. Within the range of the visible spectrum, the optimal average transmission value falls between 20% and 60%. The Tauc relation was used to determine the optical energy-band gap (Eg), which exhibited an increase from 2.93 eV to 3.11 eV upon ZnO doping. The Mn: ZnO thin films show versatile optical properties that are essential for various applications, including transparent electromagnetic interference (EMI) shielding materials, photovoltaic, and solar cells. The Mn:5%ZnO sample produced an optical band gap of 3.06 eV, which was lower than the optical band gap of 3.37 eV observed in pure ZnO films.

Keywords: CSP, MnO: ZnO, XRD, FESEM, and Spectrophotometer.

1. Introduction

The information extracted from the investigation allows the development of novel device concepts. Evaluating a new system may begin with the assumption of a flawless structure, but there is no perfect material. Scientists of semiconductors seek to achieve a superior system with the ideal material[1]. Therefore, material science and engineering aims to generate new materials with exceptional physical, chemical, and mechanical properties or modify the properties of existing materials for use in manufacturing. Thin-film research is essential because it allows for a thorough understanding of physical properties and the evaluation of devices for possible technological advancement[2]. MnOx, or manganese oxides, are a highly potent type of naturally occurring oxidant that can oxidize a variety of organic contaminants, such as phenols[3, 4]. The manganese oxide electrode exhibits excellent performance as a supercapacitor, with high efficiency, long-term durability, and remarkable corrosion resistance. This makes it the most prospective candidate for the development of commercial supercapacitors[4]. A range of synthetic techniques have been employed to produce MnO with MnO ZnO thin films. These techniques include sol–gel dipping and drop coating[5], solution-based chemical routes[6], electrostatic spray deposition[7], physical vapor deposition followed by electrochemical oxidation[8], and electrochemical deposition. One cost-effective and low-temperature soft chemical solution method is the successive ionic layer absorption and reaction (SILAR) method[9]. Additionally, atmospheric pressure chemical vapor deposition[10], and chemical spray pyrolysis techniques are also utilized[11]. Chemical spray pyrolysis (CSP) is a method used to deposit thin films by applying a solution onto a heated surface. During this process, the constituents of the solution undergo a chemical reaction, resulting in the production of a specific chemical compound. The selection of chemical reactants is crucial in CSP, as they should be chosen in a way that any other products formed during the reaction are easily evaporated at the temperatures used for deposition. The application of CSP has been widely employed for many years to deposit transparent MnO electrical conductors onto glass substrates, making it particularly advantageous for oxide deposition[12]. The CSP technique, a procedure that is relatively new and has received limited research attention, involves

* Corresponding author
E-mail address: adnan.mahmud@garmian.edu.krd (Instructor).
Peer-reviewed under the responsibility of the University of Garmian.

sequential reactions occurring on the surface of the substrate. By conducting rinsing after each reaction, heterogeneous reactions can take place when there is interaction between the solid phase and solvated ions in a solution.[13].

The current research employs various weight percentages of ZnO doping in MnO. Additionally, it investigates the level of crystallinity in the deposited thin films. The study also examines the morphological properties and stress in these films, focusing on the alteration of crystallite shapes and distribution, which may occur with a rise in crystallite size[14]. The optical and electrical properties of MnO:ZnO thin films are influenced by the distribution of crystallite sizes and the roughness of the surface[15,16]. Furthermore, the optical transparency (T) and absorption coefficient (α) are affected by the thickness of the film, which in turn impacts the optical band gap[14]. The objective of this study is to investigate the impact of varying thicknesses of MnO:ZnO thin films on their structural, optical, and electrical characteristics, specifically their applications in optics. Various techniques were employed in this study, including (CSP), X-ray diffraction (XRD), and field emission scanning electron microscope (FESEM) techniques. These techniques were used to investigate the synthesis of MnO and MnO ZnO nanostructure thin films, conduct a wettability test, and analyze optical absorbance.

2. Sample Preparation

Using chemical spray pyrolysis (CSP), MnO, Mn:5%ZnO, and Mn:10%ZnO nanostructured thin films were successfully fabricated on glass substrates. The cleansing procedure is an essential aspect of experimental research. Several steps are required to ensure that the surface of the glass substrate is free of impurities during the cleansing process. The impurities would reduce the precision of measurements for thin coatings deposited by deposition. First, a substrate of soda lime glass was used to fabricate thin coatings with a surface area of 1.7×2 cm^2. The glass substrate is held with special forceps, immersed in a receptacle containing ethanol of 99% purity, and then placed in an ultrasonic cleaner for 20 minutes to remove any remaining plankton. It will then be immersed in pure acetone solution to ensure that all impurities have been removed. After the preceding stages, the glass substrate was cleaned with distilled water before being exposed to air for curing. Finally, the substrate will be placed on the heater for 15 minutes to adjust the heat of the substrate uniformly.

The matrix solution of MnO-ZnO doped thin films was prepared using an aqueous solution comprising 1 M of Manganese (II) chloride tetrahydrate [$MnCl_2.4H_2O$] 98% Bio. Chemopharma, France, and 100 ml of deionized water. To prepare the doping substance, Zinc acetate $Zn(CH\ COO)_2(H_2O)_2$ (dehydrate) 98.5% 219.5 g/mol England.

Throughout the deposition process, the temperature of the substrate was maintained at 400ºC. During the deposition process, the carrier gas used was airflow, and a distance of 26 cm was maintained between the substrate and nozzle. The substrate temperature was consistently maintained at 400°C. The carrier gas used throughout was airflow, and a distance of 26 cm was maintained between the substrate and nozzle. The spraying time, rate, and interval between the two spray procedures were 8 seconds, 5 milliliters per minute, and two minutes, respectively. Gravimetric calculations determined the thickness of the films to be approximately 325±30 nm.

3. Characterization Methods

Manganese oxide MnO, Mn:5%ZnO, and Mn:10%ZnO nanostructured thin films were characterized using X-Ray diffraction (XRD) model: Analytical Philips (XPERT-PRO) equipped with CuKα (= 1:54178) at a generator voltage of 40 kV and a current of 10 mA. The thickness of the thin film was measured using the FE-SEM technique. This was achieved by capturing cross-section images of the film, both from a side view and a top view. This technique is utilized by the Dektak surface. Iran's Petronic Company employs VEECO Dektak for its profilometers. This technique was implemented during FE-SEM imaging to determine the surface morphology and the thickness of a portion of the deposition layers of the thin film. The optical measurements at room temperature consisted of (Absorption) and (Transmittance) measurements of the materials. The measurements were conducted using the Shimadzu Co.'s double-beam UV-visible spectroscopy model 2600, within a wavelength range of 200 to 1100 nm.

4. Results and Discussions

4.1. X-ray diffraction (XRD)

The XRD patterns of nanostructured thin films of MnO, Mn:5%ZnO, and Mn:10%ZnO were prepared using the (CSP) method as depicted in Figure (1).

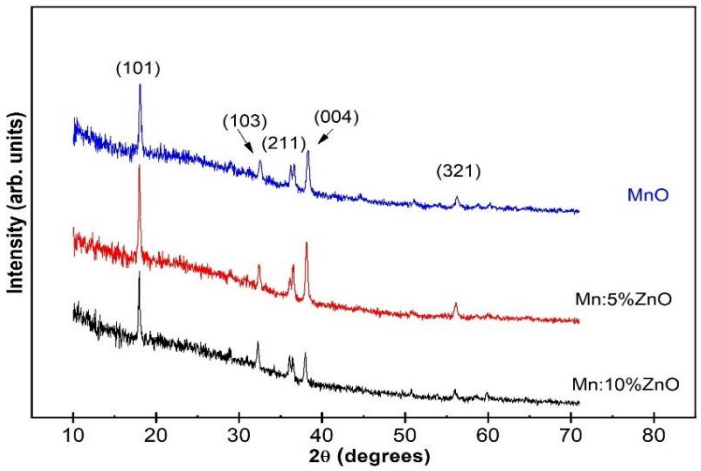

Figure 1: The XRD patterns of MnO, Mn:5%ZnO, and Mn:10%ZnO thin films.

The X-ray diffraction analysis showed the presence of peaks in the 2θ range of 10°-80°, suggesting that the thin films' intensity increases with higher levels of MnO doping in ZnO. Specifically, the diffraction peaks correspond to crystallographic planes [101], [103], [211], [004], and [321], as determined by the x-ray analysis at positions 2θ = 18.15°, 32.53°, 36.19°, 38.1°, and 58.7°, respectively. The MnO thin film sample displays Bragg reflections in its diffractogram, indicating a polycrystalline tetragonal structure. This result is confirmed by referencing standard ICSD card No (95330). Whoever the dominant pick yields when the thin film directions [101] with the

position 2θ =18.15. XRD analysis revealed that the crystallite size of nanostructured MnO, Mn:5%ZnO, and Mn:10%ZnO thin films can be calculated using the Full Width at Half Maximum (FWHM) from Scherrer's equations[15].

$$D = \frac{0.9\,\lambda}{\beta \cos\theta} \quad (1)$$

Where D is the size of the crystallites, λ is the X-ray wavelength, θ is the Bragg diffraction angle, and β is the half-maximum width. For these nanostructured thin film samples, the crystallites' size was between 29.38 and 29.62 nm (see Table 1).

Table 1: XRD results of MnO, Mn:5%ZnO, and Mn:10%ZnO nanostructured thin film.

Samples	2θ (deg)	[hkl]	d (Å)	FWHM (deg)	D (nm)	Average D (nm)
MnO	17.95	101	0.22	0.00383	17.9575	29.38
	32.25	103	0.2	0.00349	32.255	
	37.95	211	0.222	0.00387	37.954	
Mn:5%ZnO	17.98	101	0.201	0.00350	17.9853	29.499
	32.39	103	0.18	0.00314	32.3937	
	38.11	211	0.251	0.00438	38.1183	
Mn:10%ZnO	18.06	101	0.211	0.00368	18.0674	29.62
	32.5	103	0.313	0.0054	32.531	
	38.28	211	0.251	0.0043	38.2884	

The Williamson-Hall equation is utilized to determine the effect of crystallite size and strain in a diffraction pattern, which also takes into account the peak broadening (β) and is derived from the following equation[16]

$$\beta \cos\theta = \frac{0.9\,\lambda}{D} 4\varepsilon \sin\theta \quad (2)$$

Where ε represents the average microstrain. The Williamson-Hall plots, as depicted in Figure (2), enable the detection of the $\beta^* \times 10^{-3}$ values against d^* ($Å^{-1}$) for all significant peaks. These plots were obtained by applying the best linear fitting method[17]. The linear plot exhibits a positive slope of 0.0004 for the sample MnO and 0.001 for the sample Mn:10%ZnO, indicating the presence of a tensile strain[18, 19]. Additionally, our findings reveal that there is a lattice expansion in the nano-tetragonal samples prepared, as indicated by the positive micro-strain results[20]. It is important to highlight that for the Mn:5%ZnO sample, the linear plot displays a negative slope (-0.0013), suggesting the existence of compressive strain within the lattice. The plots exhibited a negative strain value for the ZnO-NPs. The observed strain, in this case, can potentially be attributed to the lattice shrinkage that was identified during the calculation of lattice parameters[17].

Figure (2. b) depicts the results of the Uniform Stress Deformation study of the Mn:5%ZnO NPs

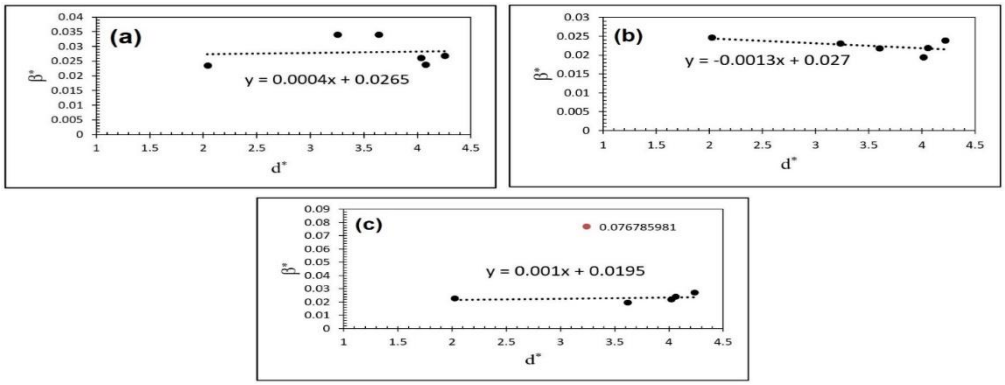

Figure 2: The W-H Plot of (a) MnO, (b) Mn:5%ZnO, and (c) Mn:10%ZnO thin films.

Table 2: W-H analysis of MnO, Mn:5%ZnO, and Mn:10%ZnO nanostructured thin film.

Samples	Average D (nm)	$\delta \times 10^{-3}$	ε
MnO	37.7	7.03	0.0004
Mn:5%ZnO	37	7.304	-0.0013
Mn:10%ZnO	52.1	3.68	0.0012

Table (2) illustrates the computations used to determine the crystallite size, microstrain (ε), and dislocation density (δ) through the following formula[21].

$$\delta = \frac{1}{D^2} \quad (3)$$

It was discovered that the value of (δ) falls as the amount of ZnO added twice to the MnO nanostructured thin films increases.

4.2 Field emission scanning electron microscope (FE-SEM)

Figure (3) illustrates the typical morphology of three types of nanostructured thin films: MnO, Mn:5%ZnO, and Mn:10%ZnO. The images labeled (a_0, a_1, a_2), (b_0, b_1, b_2), and (c_0, c_1, c_2) represent these films, respectively. Through an analysis of the differences and arrangements in the texture of the films, it becomes clear that the addition of zinc nitrate to manganese leads to a significant augmentation in the thickness of the thin film. More specifically, as the concentration of zinc nitrate increases from 0% to 5% and 10%, the thickness of the thin film also increases. The images obtained through FE-SEM show distinct changes in crystallite size, which are dependent on the specific method of doping used. Figure 2 displays the low and high-magnification images of MnO, Mn:5%ZnO, and Mn:10%ZnO nanostructured thin films. The images depict tetragonal morphology and pointed tips in certain instances. Moreover, the doping level has an impact on the crystallite structure of the film surface. In the case of undoped MnO, the surface consists of nanostructures composed of particles of uniform size, exhibiting minimal presence of pin holes (as depicted in Figure (3. a)). The optimal Mn:5%ZnO thin film sample showed a surface without any cracks. However, the surface appeared unevenly modified, with structures consisting of interconnected particles of varying sizes. The surface plane of the thin film structure showed an improvement in evenness compared to the initial state (as depicted in Figure (3. b)). By contrast, the ZnO-doped Mn thin films (with Zn doping levels of 5% and 10% by weight) exhibited a smooth and uniform surface. The structures within these films were tightly packed and had equally sized crystallites (as seen in Figure. (3b,c)). When the Zn doping concentration was further increased to 10% by weight, the surface underwent modification characterized by the presence of equal-sized particle structures and numerous pinholes. These findings suggest that the addition of Zn to pure MnO slightly deteriorated the surface morphology, but subsequent Zn doping led to a modification of the surface, which aligns with the results obtained from the XRD analysis. On the other hand, it is worth mentioning to note that the change in the doped process affects the properties of the films[22]. The thickness of the thin films for MnO, Mn:5%ZnO, and Mn:10%ZnO was determined by analyzing the cross-section side view images obtained from FESEM, as shown in (Figure. (3 a_2, b_2, and c_2)). It clearly shows that the thickness decreases by increasing the amount of ZnO to the structure of MnO thin films from 759.2nm, 452.2 nm, and 350.6nm respectively. The impact of adding ZnO dopants on the structural, morphological, and optical characteristics of MnO thin films was investigated through the utilization of the (CSP) method. K,

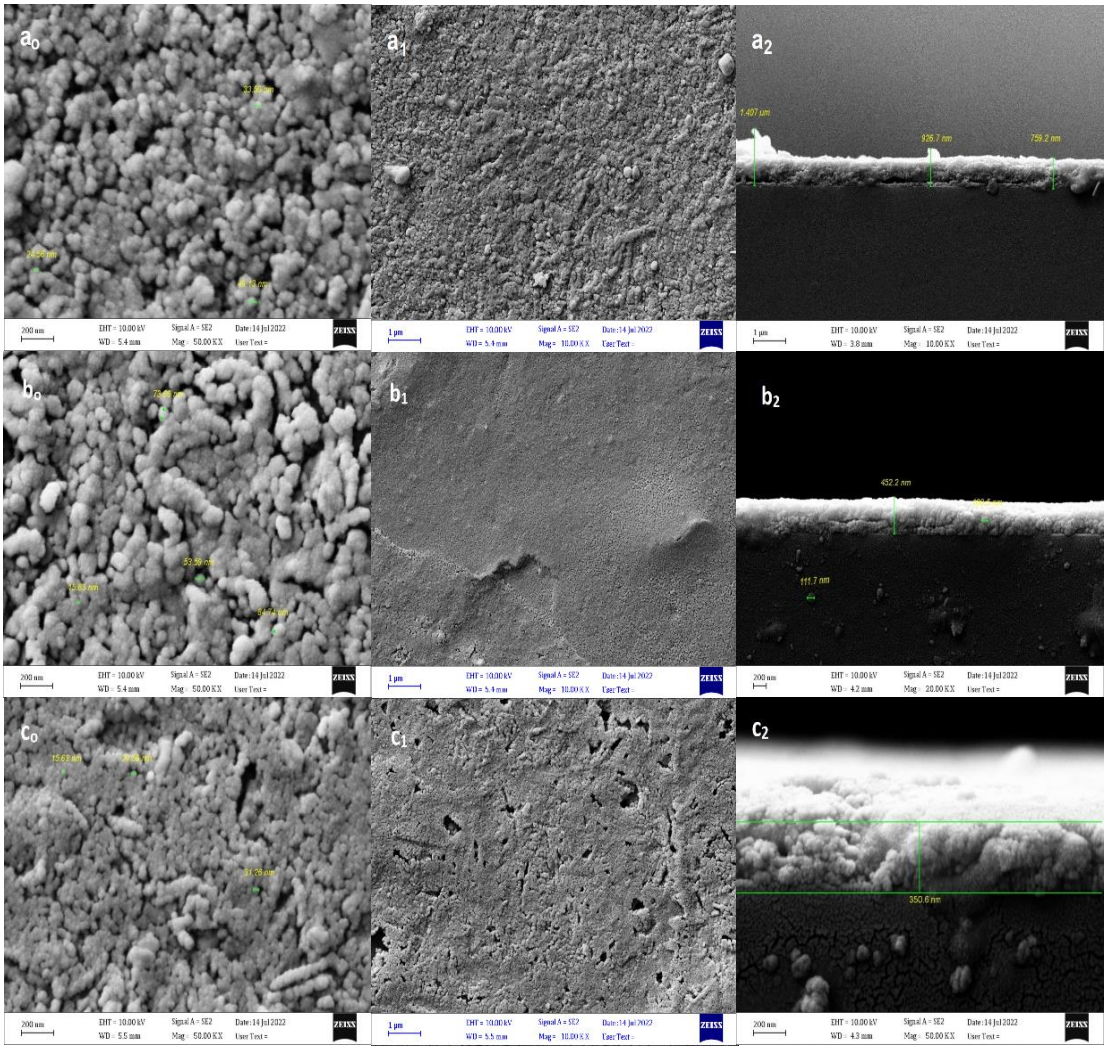

Figure 3: The top and side view FE-SEM image of MnO, Mn:5%ZnO, and Mn:10%ZnO thin films labeled (a0, a1, a2), (b0, b1, b2), and (c0, c1, c2) respectively.

4.3 Energy dispersive X-ray spectroscopy (EDS)

The level of purity observed in the MnO nanostructure thin films is influenced by two primary factors: the composition of the spry solution and the temperature of the substrate[23]. To investigate the influence of these factors on the purity of MnO nanostructure thin films, energy-dispersive X-ray spectroscopy (EDS) was employed. EDS is a frequently used analytical technique for conducting elemental analysis. The deposition samples obtained using CSP techniques at a substrate temperature of 400ºC were analyzed for elemental composition using Energy Dispersive Spectroscopy (EDS), as shown in Figure 4 (a,b,c). The analysis indicated the presence of Mn, Zn, and oxygen in the Mn:5%ZnO sample. These findings support the results obtained from FE-SEM and X-ray diffraction analyses, providing further evidence for the exceptional quality of this thin film in terms of its crystallite size, grain size, particle size, and porosity when compared to samples prepared using alternative methods.

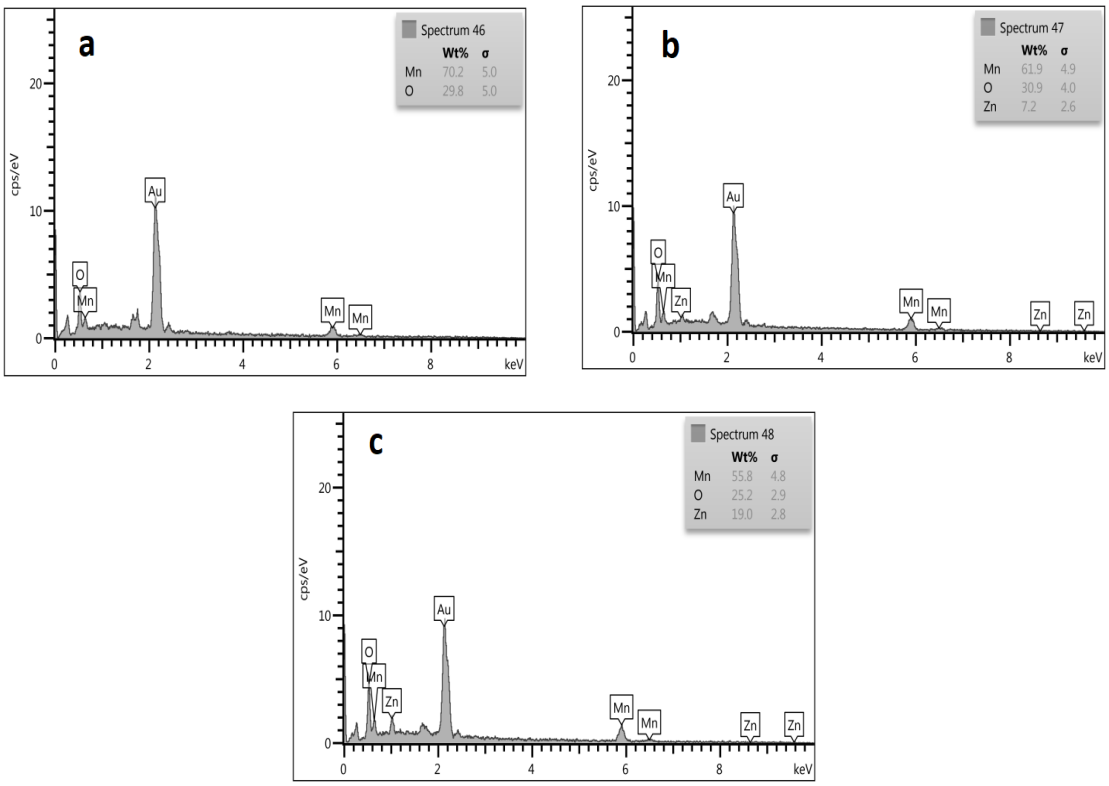

Figure 4: EDX spectra of (a) MnO, (b) Mn:5%ZnO, and (c) Mn:10%ZnO thin films.

The ratio of Mn:Zn and the amount of oxygen on the surface of thin films illustrated in Table (3)

Table 3: The ratio of Mn, Zn, and oxygen on the surface of nanostructure thin films prepared by the CSP technique.

Samples	Mn Wt%	Zn Wt %	O Wt %
MnO	70.2	-	29.8
Mn:5%ZnO	61.9	7.2	30.9
Mn:10%ZnO	55.8	19	25.2

4.4 Optical study

To evaluate the optical properties of nanostructured MnO, Mn:5%ZnO, and Mn:10%ZnO thin films. Transmission, absorption coefficient, and band gap energy of undoped MnO and ZnO-doped MnO thin films are examined. The experimental measurements are carried out at room temperature, with a particular focus on the significant absorbance observed in the visible region.[24]. At the normal temperature, UV-vis absorption and transmission spectra of the samples were obtained. Figure (5.a) depicts the optical transmittance spectra of nanostructured MnO, Mn:5%ZnO, and Mn:10%ZnO thin films. The findings indicate that the transmittance values of the samples ranged from 20 to 60 percent. Notably, the wavelength ranges of 100-1100 nm exhibited the maximum transmittance. Conversely, a higher concentration of doping led to a reduction in transmittance. The decrease in transmittance can be attributed to an elevation in defect concentration and the presence of extra crystallite boundaries[25]. To calculate the absorption coefficient (α) of MnO, Mn:5%ZnO, and Mn:10%ZnO nanostructures, the following equation is commonly used:

$$\alpha = 2.303\frac{A}{t} \quad (4)$$

In this equation, α represents the absorption coefficient, t denotes film-thickness, and A represents the absorbance. The absorption coefficient provides information about the extent to which the material absorbs light at a given wavelength. Using the obtained

values of the absorption coefficient, it is possible to analyze the absorption behavior of the samples and assess their optical characteristics.

In Figure (5b), it is clear that the absorption coefficient (α) exhibits an upward trend with increasing doping concentration. This phenomenon leads to a heightened generation of levels that are concentrated within the energy gap. The functioning of this mechanism involves a reduction in the energy gap values, which leads to a displacement of the absorption edge towards longer wavelengths. As the occurrence of doping escalates, there is a corresponding augmentation in the density of charged atoms. Consequently, each electron becomes enveloped by exchange and correlation holes, leading to a diminution in the electron's energy and a subsequent reduction in the conduction band[26].

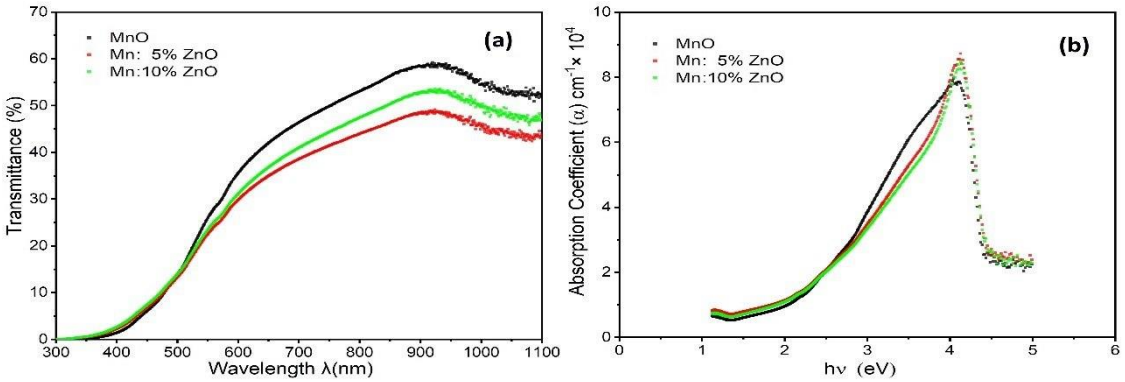

Figure 5: (a) Transmittance and (b) absorption coefficient of MnO, Mn:05%ZnO, and Mn:10%ZnO nanostructured thin films.

The Tauc formula is a frequently used method for determining the magnitude of the optical energy gap[27].

$$(\alpha h\nu) = A\left(h\nu - E_g\right)^n \quad (5)$$

In the given context, α represents the absorption coefficient, h denotes Planck's constant, and A represents a constant value. The energy band gap, denoted as Eg, and the quantum selection rules for each material determine the value of n. For the direct band gap, n can be equal to 1/2, while for the indirect band gap, n can be equal to 2. The choice of n=1/2 was made due to its ability to produce a highly accurate linear fit curve within the band-edge region. The determination of the band gap energy is achieved in Figure (6) through the establishment of a correlation $(h\nu)^2$. Subsequently, a straight line is drawn to the linear segment of the curve at the point where $(h\nu)^2$ equals zero, intersecting the axis representing the photon energy.

Increasing the concentration of ZnO doping resulted in direct transitions being promoted and new localized levels, particularly donor levels, being developed. This was indicated by the intersection of the x-axis, which reflected the value of the optical band gap. These levels are situated beneath the conduction band and are prepared to accept electrons and generate tails of localized energy within the optical energy gap by absorbing photons with low-lying energy (shifted absorption edge towards long wavelengths), thereby increasing the optical energy-gaps value[28]. The observed increases in band gap in ZnO-doped MnO materials may be due to the presence of Zn metal ions, which influence the optical-band gap.

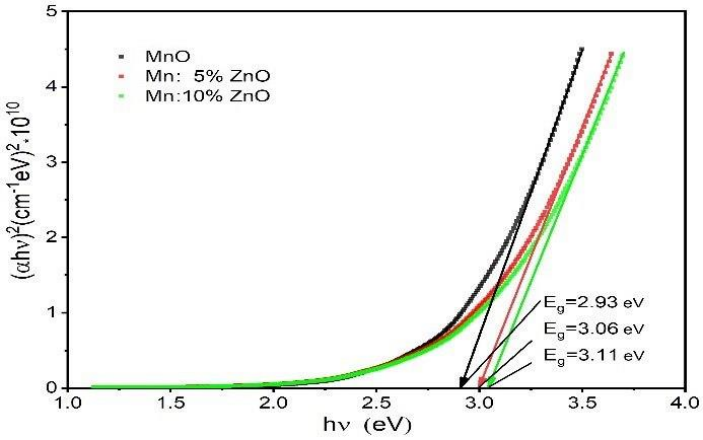

Figure 6: The direct optical band gap (E_g) of MnO, Mn:5%ZnO, and Mn:10%ZnO nanostructured thin films.

Table4 : The data of band gaps(eV), transmittance %, and Absorption coefficient (α) for MnO, Mn:5%ZnO, and Mn:10%ZnO nanostructured thin film.

Samples	Band gaps(ev)	Transmittance%	Absorption coefficient (α)$cm^{-1}\times10^4$
MnO	2.93	60	8
Mn:5%ZnO	3.06	50	9
Mn:10%ZnO	3.11	55	8.5

The findings derived from the data presented in Table 4 demonstrate a distinct correlation between the optimal condition for the Mn:5%ZnO samples and their highest absorbance

coefficient (α). This observation holds significant value in the context of sample preparation. The term "photovoltaic" refers to a device known as a solar cell[29, 30].

Conclusions

The chemical spray pyrolysis method was utilized to fabricate nanostructured thin films with a tetragonal polycrystalline structure. The films were composed of MnO, Mn:5%ZnO, and Mn:10%ZnO. The Sherer equation, which is applied in X-ray diffraction (XRD) analysis, shows that the doping of MnO with ZnO causes a slight growth in crystallite size. Specifically, the crystallite sizes were measured to be 29.39 nm, 29.49 nm, and 29.62 nm for the MnO, Mn:5%ZnO, and Mn:10%ZnO nanostructured thin films, respectively. In addition to investigate the impact of doped ZnO, micro strain experiments were conducted using the Williamson–Hall method. FE-SEM images demonstrated that as the mixture concentration increases, so does the growth of deposition on the substrate. This result is in excellent accord with the outcome of the XRD analysis. It clearly shows that the thickness decreases by increasing the amount of ZnO in the structure of MnO thin films. Transparency ranges from 20 to 60 percent, with a maximum in the wavelength range (100-1100 nm) and a decrease with increasing doping concentration for all films, particularly in the VIS region. The increase in ZnO doping causes a progressive increase in the vis region's indue absorption. The introduction of ZnO doping has caused a red shift in the optical band gap, increasing it from 2.93 eV to 3.11 eV.

Conflict of interests

The authors declare that they have no known competing financial interests or personal relationships that could be perceived as having influenced the work described in this paper.

Acknowledgments

The author is grateful to the research lab at the College of Education, University of Garmian, and the Day Petronic company for providing the characterization facility.

Funding details

No financial support was provided for the research, authoring, or publication of this article.

References

1. W. H. Weber, and R. Merlin, *Raman scattering in materials science*: Springer Science & Business Media, 2000.
2. S. M. Sze, and M.-K. Lee, *Semiconductor Devices: Physics and Technology: Physics and Technology*: Wiley Global Education, 2012.
3. C. K. Remucal, and M. Ginder-Vogel, "A critical review of the reactivity of manganese oxides with organic contaminants," *Environmental Science: Processes & Impacts,* vol. 16, no. 6, pp. 1247-1266, 2014.
4. A. T. Stone, "Reductive dissolution of manganese (III/IV) oxides by substituted phenols," *Environmental Science & Technology,* vol. 21, no. 10, pp. 979-988, 1987.
5. M. Elias, M. N. Uddin, J. K. Saha, M. A. Hossain, D. R. Sarker, S. Akter, I. A. Siddiquey, and J. Uddin, "A highly efficient and stable photocatalyst; N-doped ZnO/CNT composite thin film synthesized via simple sol-gel drop coating method," *Molecules,* vol. 26, no. 5, pp. 1470, 2021.
6. K. Choy, "Chemical vapour deposition of coatings," *Progress in materials science,* vol. 48, no. 2, pp. 57-170, 2003.
7. K. Mahmood, B. S. Swain, and H. S. Jung, "Controlling the surface nanostructure of ZnO and Al-doped ZnO thin films using electrostatic spraying for their application in 12% efficient perovskite solar cells," *Nanoscale,* vol. 6, no. 15, pp. 9127-9138, 2014.
8. M. Li, J. Zhai, H. Liu, Y. Song, L. Jiang, and D. Zhu, "Electrochemical deposition of conductive superhydrophobic zinc oxide thin films," *The Journal of Physical Chemistry B,* vol. 107, no. 37, pp. 9954-9957, 2003.
9. V. L. Patil, S. A. Vanalakar, P. S. Patil, and J. H. Kim, "Fabrication of nanostructured ZnO thin films based NO2 gas sensor via SILAR technique," *Sensors and Actuators B: Chemical,* vol. 239, pp. 1185-1193, 2017.
10. S. Jung, N. Imaishi, and H. Park, "ZnO thin films growth by APCVD using zinc acetate; Sakusan aen wo genryo to suru ZnO usumaku no APCVD," *Kagaku Kogaku Ronbunshu,* vol. 21, 1995.
11. M. Kumar, B. Singh, P. Yadav, V. Bhatt, M. Kumar, K. Singh, A. Abhyankar, A. Kumar, and J.-H. Yun, "Effect of structural defects, surface roughness on sensing properties of Al doped ZnO thin films deposited by chemical spray pyrolysis technique," *Ceramics International,* vol. 43, no. 4, pp. 3562-3568, 2017.
12. J. B. Mooney, and S. B. Radding, "Spray pyrolysis processing," *Annual review of materials science,* vol. 12, no. 1, pp. 81-101, 1982.
13. D. Dubal, D. Dhawale, R. Salunkhe, S. Pawar, and C. Lokhande, "A novel chemical synthesis and characterization of Mn3O4 thin films for supercapacitor application," *Applied Surface Science,* vol. 256, no. 14, pp. 4411-4416, 2010.
14. V. Kumar, N. Singh, R. Mehra, A. Kapoor, L. Purohit, and H. Swart, "Role of film thickness on the properties of ZnO thin films grown by sol-gel method," *Thin solid films,* vol. 539, pp. 161-165, 2013.
15. G. W. Scherer, "Use of the Adam-Gibbs equation in the analysis of structural relaxation," *Journal of the American Ceramic Society,* vol. 67, no. 7, pp. 504-511, 1984.
16. S. Mustapha, M. Ndamitso, A. Abdulkareem, J. Tijani, D. Shuaib, A. Mohammed, and A. Sumaila, "Comparative study of crystallite size using Williamson-Hall and Debye-Scherrer plots for ZnO nanoparticles," *Advances in Natural Sciences: Nanoscience and Nanotechnology,* vol. 10, no. 4, pp. 045013, 2019.
17. A. K. Zak, W. A. Majid, M. E. Abrishami, and R. Yousefi, "X-ray analysis of ZnO nanoparticles by Williamson–Hall and size–strain plot methods," *Solid State Sciences,* vol. 13, no. 1, pp. 251-256, 2011.
18. R. Tholkappiyan, and K. Vishista, "Combustion synthesis of Mg–Er ferrite nanoparticles: cation distribution and structural, optical, and magnetic properties," *Materials Science in Semiconductor Processing,* vol. 40, pp. 631-642, 2015.
19. Z. T. Khodair, A. A. Khadom, and H. A. Jasim, "Corrosion protection of mild steel in different aqueous media via epoxy/nanomaterial coating: preparation, characterization and mathematical views," *Journal of Materials Research and Technology,* vol. 8, no. 1, pp. 424-435, 2019.
20. S. Sarkar, and R. Das, "Determination of structural elements of synthesized silver nano-hexagon from X-ray diffraction analysis," 2018.
21. D. Aryanto, W. Jannah, T. Sudiro, A. Wismogroho, P. Sebayang, and P. Marwoto, "Preparation and structural characterization of ZnO thin films by sol-gel method." p. 012025.
22. A.-I. Istrate, I. Mihalache, C. Romanitan, O. Tutunaru, R. Gavrila, and V. Dediu, "Copper doping effect on the properties in ZnO films deposited by sol–gel," *Journal of Materials Science: Materials in Electronics,* vol. 32, pp. 4021-4033, 2021.
23. K. Ukoba, A. Eloka-Eboka, and F. Inambao, "Review of nanostructured NiO thin film deposition using the spray pyrolysis technique," *Renewable and Sustainable Energy Reviews,* vol. 82, pp. 2900-2915, 2018.
24. G. Kaur, A. Mitra, and K. Yadav, "Pulsed laser deposited Al-doped ZnO thin films for optical applications," *Progress in Natural Science: Materials International,* vol. 25, no. 1, pp. 12-21, 2015.
25. P. Parent, C. Laffon, I. Marhaba, D. Ferry, T. Regier, I. Ortega, B. Chazallon, Y. Carpentier, and C. Focsa, "Nanoscale characterization of aircraft soot: A high-resolution transmission electron microscopy, Raman spectroscopy, X-ray photoelectron and near-edge X-ray absorption spectroscopy study," *Carbon,* vol. 101, pp. 86-100, 2016.

26. X. Lu, D. T. Morelli, Y. Xia, and V. Ozolins, "Increasing the thermoelectric figure of merit of tetrahedrites by co-doping with nickel and zinc," *Chemistry of Materials,* vol. 27, no. 2, pp. 408-413, 2015.

27. S. Hong, E. Kim, D.-W. Kim, T.-H. Sung, and K. No, "On measurement of optical band gap of chromium oxide films containing both amorphous and crystalline phases," *Journal of non-crystalline solids,* vol. 221, no. 2-3, pp. 245-254, 1997.

28. H. Zeyada, M. El-Nahass, I. Elashmawi, and A. Habashi, "Annealing temperatures induced optical constant variations of methyl violet 2B thin films manufactured by the spin coating technique," *Journal of non-crystalline solids,* vol. 358, no. 3, pp. 625-636, 2012.

29. K. L. Chopra, S. R. Das, K. L. Chopra, and S. R. Das, *Why thin film solar cells?*: Springer, 1983.

30. P. Prepelita, R. Medianu, B. Sbarcea, F. Garoi, and M. Filipescu, "The influence of using different substrates on the structural and optical characteristics of ZnO thin films," *Applied surface science,* vol. 256, no. 6, pp. 1807-1811, 2010.